

Microrheology of Wormlike Micellar Fluids from the Diffusion of Colloidal Probes

P. A. Hassan,^{†*} K. Bhattacharya,[‡] S. K. Kulshreshtha,[†] and S. R. Raghavan[§]

Novel Materials and Structural Chemistry Division and Applied Chemistry Division, Bhabha Atomic Research Center, Trombay, Mumbai 400 085, India, and Department of Chemical Engineering, University of Maryland, College Park, Maryland 20742

Received: December 15, 2004; In Final Form: March 2, 2005

The microrheology of cationic micellar solutions has been investigated as a function of added organic salts using quasielastic light scattering (QELS). Two organic salts, sodium *p*-toluene sulfonate and sodium salicylate, were used to induce microstructural changes in cetyl trimethylammonium bromide (CTAB) micelles. The mean-squared displacement (MSD) of polystyrene probe particles embedded in CTAB micellar solutions was monitored by QELS in the single-scattering regime. Through the use of the generalized Stokes–Einstein relationship, the frequency-dependent complex shear moduli of each fluid were estimated from the Laplace transform of the corresponding MSD. The salt-induced transition from nearly spherical to elongated wormlike micelles and consequent changes in fluid response from viscous to viscoelastic are clearly captured by microrheology.

Introduction

During the past few years, several complementary techniques have been developed for probing the rheological properties of complex fluids at a microscopic length scale, an area that has come to be called microrheology.¹ Typically, the technique relies on measuring the local displacement of embedded colloidal probe particles and converting this displacement into macroscopic rheological properties. The driving force for particle displacement can arise either from random Brownian (thermal) forces acting on the probe^{2–5} or from an externally imposed force such as a magnetic field.^{6,7} Application of external fields, however, may induce substantial strains in the probe particles and may hence correspond to a nonlinear fluid response. In contrast, the strains resulting from thermal probe motion are quite low, and thus a linear response is ensured. Microrheology provides new insight into the presence of local inhomogeneities in materials, and the results are often complementary to the macrorheology of the fluid obtained from conventional mechanical rheometry. Microrheological experiments can be performed on relatively small sample volumes as compared to those required for macrorheology, and this can be a major advantage in characterizing many costly biological fluids. Moreover, this technique can be used to probe complex moduli over an extended frequency range that is inaccessible by conventional rheometry.

Thermally driven diffusion of colloidal probe particles in complex fluids such as polymer solutions and surfactant assemblies has been of long-standing interest.^{8–15} Different approaches have been employed for measuring the time-dependent mean-squared displacement (MSD) of colloidal particles. These include laser deflection particle tracking (LDPT),³ atomic force microscopy (AFM),^{16–18} optical inter-

ferometry,⁵ epifluorescence microscopy,¹⁹ and dynamic light scattering (DLS).^{2,20,21} DLS has been used both in the single-scattering limit^{20,21} (quasielastic light scattering (QELS)) and in the multiple-scattering regime, i.e., diffusing wave spectroscopy (DWS).^{2,22} In this paper, we will use QELS in the single-scattering regime to measure the MSD of colloidal probes in our samples.

The samples of interest are based on a cationic surfactant and an organic salt. These belong to a class of surfactant systems that form long flexible wormlike micelles in solution, resulting in viscoelastic behavior of the fluid.^{23–28} Salts with hydrophobic counterions are known to induce micellar growth at very low concentrations due to their tendency to adsorb on the surface of ionic micelles. Typical hydrophobic salts for cationic micelles include sodium *p*-toluene sulfonate (SPTS),²⁵ sodium salicylate (SS),^{29,30} and sodium 3-hydroxynaphthalene-2-carboxylate (SHNC).³¹ The rheological properties of entangled wormlike micellar solutions are similar to those of semidilute polymer solutions with the difference that the micelles are dynamic in nature (breaking and recombining rapidly).^{32,33} Wormlike micelles can thus be viewed as substitutes for polymers in applications that require thickening or drag reduction.^{34,35} For example, wormlike micellar solutions are currently being used as hydraulic fracturing fluids for enhanced oil recovery.

The basic theory of dynamics and rheology of wormlike micelles was originally developed by Cates and co-workers as an extension of the reptation model for polymer dynamics. According to this theory, the dynamics and rheology depend on two different time scales of the system, i.e., the reptation time (τ_r) and the breaking time (τ_b). When $\tau_b \gg \tau_r$, stress relaxation occurs by a stretched exponential in time, as expected for a solution of polydispersed polymers. However, when $\tau_b \ll \tau_r$, the stress relaxation behavior follows a single exponential, much like for a Maxwell fluid. Macroscopic rheological measurements on several wormlike micellar fluids are consistent with the predictions of the Cates model.

Studies on probe diffusion and microrheology have been conducted in several viscoelastic fluids, mostly polymeric.^{36–39}

* Author to whom correspondence should be addressed. Phone: +91-22 25592327. Fax: +91-22 25505151. E-mail: hassan@apsara.barc.ernet.in.

[†] Novel Materials and Structural Chemistry Division, Bhabha Atomic Research Center.

[‡] Applied Chemistry Division, Bhabha Atomic Research Center.

[§] Department of Chemical Engineering, University of Maryland.

There are only a few studies, however, on the microrheology of wormlike micellar solutions.^{40–42} The present study is an attempt to elucidate the microrheology of micellar solutions using QELS. We focus on a cationic micellar system formed by the surfactant, cetyl trimethylammonium bromide (CTAB). The effect of organic additives (SPTS and SS) on these cationic micelles, in terms of promoting the growth of flexible cylinders, is inferred from microrheology.

Materials and Methods

CTAB and SPTS were obtained from Sigma, and SS is from Fluka. Standard polystyrene (PS) beads of radius 100 nm were obtained from Duke Scientific. Micellar solutions containing surfactant and salt were prepared in dust-free Nanopure water (Millipore). The PS probe particles were added to the solutions, and the resulting samples were kept overnight for equilibration. The concentration of PS particles was kept constant in all samples. This concentration was chosen in such a way that the intensity scattered by the particles was approximately 50 times higher than that from the micellar solution. The scattered intensity correlation functions were measured using a Malvern 4800 autosizer employing a 7132 digital correlator. The light source was an argon-ion laser (514.5 nm) operated at 10 mW laser power. The scattering angle was maintained at 90°. All measurements were carried out at 25 °C.

Theory

The MSD of probe particles embedded in surfactant solutions can be obtained from QELS measurements as follows. In QELS, the first-order electric-field autocorrelation function, $g^{(1)}(\tau)$ is related to the MSD, $\Delta r^2(\tau)$, by the relation

$$g^{(1)}(\tau) = \exp\left(-\frac{1}{6}q^2\Delta r^2(\tau)\right) \quad (1)$$

where q is the magnitude of the scattering vector and is given by $q = 4\pi n/\lambda \sin(\theta/2)$, with n being the refractive index of the solvent, λ the wavelength of light, and θ the scattering angle. In practice, the measured quantity is the time-averaged intensity autocorrelation function $g^{(2)}(\tau)$, which for photocounts obeying Gaussian statistics can be related to $g^{(1)}(\tau)$ by the Siegert relation⁴³

$$g^{(2)}(\tau) = \beta + A|g^{(1)}(\tau)|^2 \quad (2)$$

where β is the baseline and A is an adjustable parameter called the coherence factor that depends on the scattering geometry.

The MSD of the particles reflects the influence of the fluid on the thermal motion of the scatterers. Assuming the complex fluid to be an isotropic, incompressible continuum around a sphere, the complex shear modulus $G(s)$ of the fluid can be obtained from the MSD using a generalized Stokes–Einstein relationship²

$$G(s) = \frac{k_B T}{\pi a s \langle \Delta r^2(s) \rangle} \quad (3)$$

where $\Delta r^2(s)$ is the Laplace transform of the MSD, $k_B T$ the thermal energy, a the radius of the probe particle, and s the Laplace frequency. The above equation assumes that the Stokes–Einstein relation valid for Newtonian fluids can be generalized to viscoelastic fluids and the inertial effects on probe motion can be neglected. Once $G(s)$ has been obtained, it can be fitted to a functional form in s , which can then be used to estimate the complex modulus $G^*(\omega)$ in the frequency (ω)

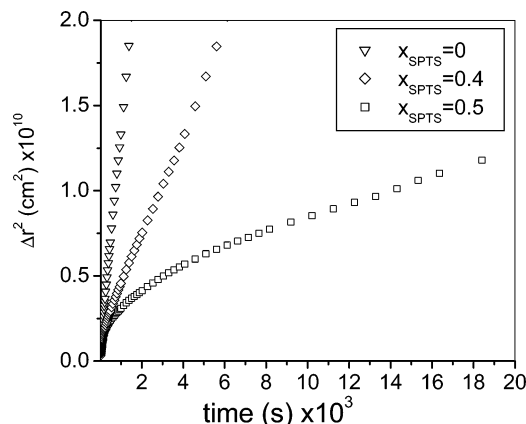


Figure 1. Variation of the mean-squared displacement, $\Delta r^2(t)$, of probe particles with time in CTAB micelles (100 mM) at different concentrations of the salt SPTS ($x_{\text{SPTS}} = [\text{SPTS}]/[\text{CTAB}]$). At low x_{SPTS} , the variation is linear, indicating the viscous nature of the fluid. Nonlinear variation is observed at high x_{SPTS} .

domain, by the method of analytic continuation² (substituting $s = i\omega$ in the fitted form). The real and imaginary parts of $G^*(\omega)$ are the storage and loss moduli of the fluid, respectively. The storage modulus G' represents the elastic component of the stress, while the loss modulus G'' represents the viscous component. For a purely viscous fluid having a viscosity η , $G^*(\omega) = i\omega\eta(\omega)$, and thus $G' = 0$ and $G'' = \eta\omega$.

Results and Discussion

We investigated the thermal motion of colloidal probe particles in micellar solutions using QELS. The concentration of the surfactant, CTAB, was fixed at 0.1 M, and the molar ratio of salt to surfactant ($x_{\text{salt}} = [\text{salt}]/[\text{CTAB}]$) was varied. At low values of x_{salt} , the micelles are nearly spherical, and the solution has a low viscosity. With an increase in salt concentration, the electrostatic repulsion between the cationic surfactant headgroups is reduced, thereby increasing the surfactant packing parameter.⁴⁴ This facilitates the growth of micelles from nearly spherical to rodlike or wormlike assemblies. When the wormlike micelles are sufficiently long, they overlap and entangle into a transient network. This causes significant changes in the rheological behavior of the fluid and affects the motion of probe particles in that fluid.

Figure 1 shows representative plots of the particle MSD, $\Delta r^2(\tau)$, at three different concentrations of the SPTS salt (x_{SPTS}). In the absence of any added salt ($x_{\text{SPTS}} = 0$), the MSD is linear in time, as expected for the random, Brownian motion of spherical particles in a Newtonian fluid. The relation between the MSD and the diffusion coefficient D of the particles is

$$\Delta r^2(\tau) = 6D\tau \quad (4)$$

Thus, from the slope of this line, we can determine the diffusion coefficient D of the particles, which is found to be 2.22×10^{-8} cm²/s. This is consistent with the value expected for spheres of 100 nm radius in water at room temperature from the Stokes–Einstein equation. At small concentrations of added salt (i.e., $x_{\text{SPTS}} < 0.4$), the MSD remains linear (data not shown). However, at higher salt concentrations ($x_{\text{SPTS}} = 0.4$ or higher), the MSD shows a nonlinear behavior as a function of time, and this is clearly seen at $x_{\text{SPTS}} = 0.5$. This nonlinear behavior indicates the restricted diffusion of the particles. Note that as time increases, the slope of the $\Delta r^2(\tau)$ curve decreases, which implies a slowing down of the particle diffusion. This can be explained by considering that under the high salt conditions, a

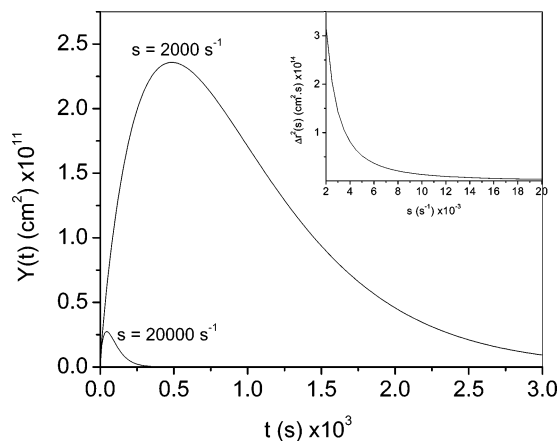


Figure 2. Representative plot of the function $Y(t)$ under the Laplace integral at two different frequencies. The area under the curve decreases with an increase in frequency. Inset shows the variation of the Laplace transform of $\Delta r^2(t)$ with frequency.

network of long micelles exists, which creates topological restrictions for particle diffusion.

The changes in MSD upon addition of salt can be correlated with corresponding changes in the fluid microrheology using the generalized Stokes–Einstein relationship, as discussed earlier. On the basis of the time scales probed in this study, we can reliably estimate the microrheology only over a limited frequency (ω) range from 2000 to 20 000 s^{-1} . This is evident from a plot of the function $Y(t)$ under the Laplace integral, where

$$Y(t) = \Delta r^2(t) e^{-st} \quad (5)$$

Figure 2 shows $Y(t)$ for $x_{\text{SPTS}} = 0$. For $s < 2000 \text{ s}^{-1}$, the function $Y(t)$ does not vanish completely within the measurement time scale, and truncation errors in numerical integration could thus arise. For $s > 20\,000$, the function is sensitive to the small time behavior of the MSD, and this can reliably be estimated only in the multiple-scattering limit, i.e., using DWS. The area under the $Y(t)$ curve gives the value of the Laplace integral $\Delta r^2(s)$, and this is shown in the inset to Figure 2.

The real (G') and imaginary (G'') parts of the complex shear modulus calculated from $\Delta r^2(s)$ are shown in Figure 3 for two salt concentrations. For $x_{\text{SPTS}} = 0$ (Figure 3a), G'' is higher than G' at all frequencies, indicating the viscous nature of the sample. Also, G' is close to zero, and G'' is linear in ω , which is expected for a Newtonian fluid. In that case, the slope of the G'' versus ω line is the viscosity of the fluid, and we find a viscosity value of 0.89 cP from this slope. This value is consistent with our measurements of the sample viscosity, and it is practically identical to the viscosity of water at this temperature. Thus, the presence of spherical micelles at low volume fractions has a negligible influence on the fluid viscosity. Next, for the sample with $x_{\text{SPTS}} = 0.5$ (Figure 3b), G' is higher than G'' , indicating the predominantly elastic nature of the sample within the indicated frequency range. The elastic behavior in this case reflects the presence of an entangled network of long micelles at this salt concentration.^{23,24}

The changes in microrheology with successive addition of salt can be visualized from a plot of the ratio G''/G' at given frequency. In mechanical rheometry, the ratio G''/G' is equal to $\tan \delta$, where δ is the phase difference between the stress and the strain. For Newtonian fluids, the phase angle δ is 90° whereas for viscoelastic fluids, δ varies between 0° and 90° . Figure 4 shows the variation of $\tan \delta = G''/G'$ as a function of x_{SPTS} at three frequencies ($\omega = 1000, 10\,000, \text{ and } 20\,000 \text{ s}^{-1}$).

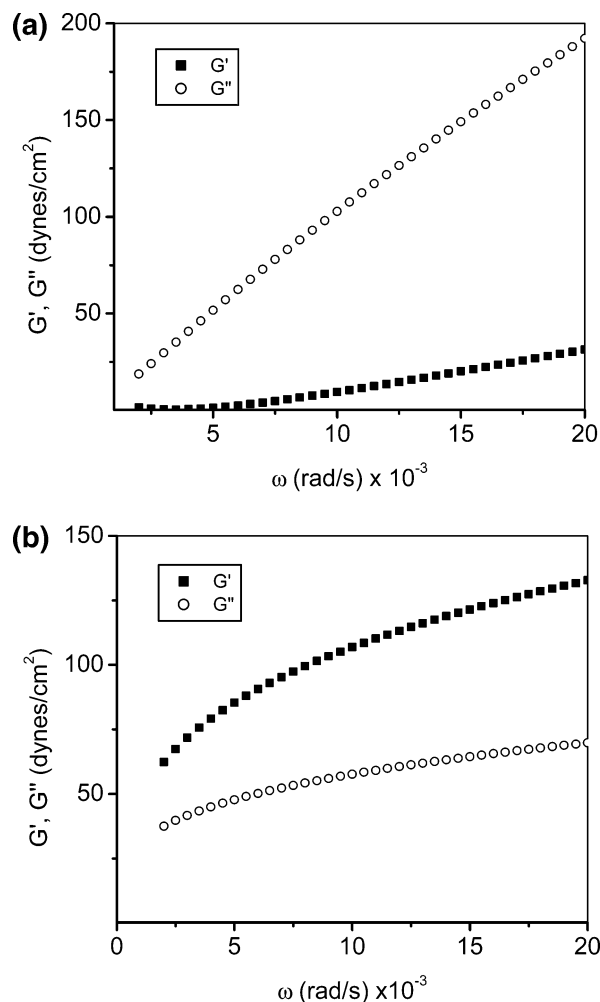


Figure 3. Variation of the storage and loss moduli with frequency for CTAB solutions containing different amounts of salt SPTS as calculated from the generalized Stokes–Einstein relation: (a) $x_{\text{SPTS}} = 0$; (b) $x_{\text{SPTS}} = 0.5$.

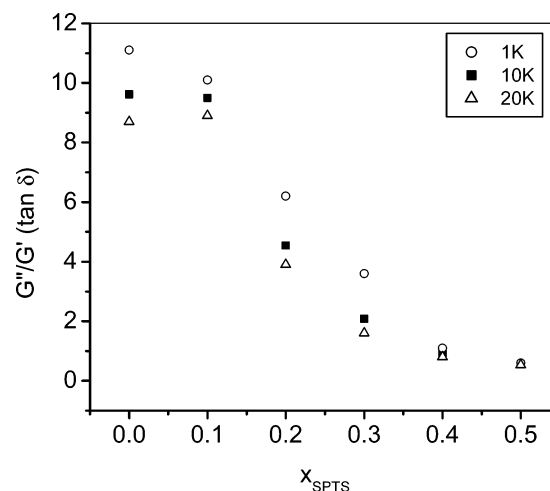


Figure 4. Changes in the ratio of G'' to G' (i.e., $\tan \delta$) at $\omega = 1000, 10\,000, \text{ and } 20\,000 \text{ s}^{-1}$ as a function of x_{SPTS} . The phase angle becomes less than 45° ($\tan \delta < 1$) at $x_{\text{SPTS}} > 0.4$, indicating predominantly elastic behavior.

Over this frequency range, $\tan \delta$ is only weakly dependent on frequency. At low salt concentrations, the value of $\tan \delta$ is ca. 10, which corresponds to a phase angle δ of 84° and indicates the viscous, Newtonian behavior of the fluid. As x_{SPTS} increases, $\tan \delta$ decreases rapidly, and at $x_{\text{SPTS}} = 0.5$, it is ca. 0.56, which

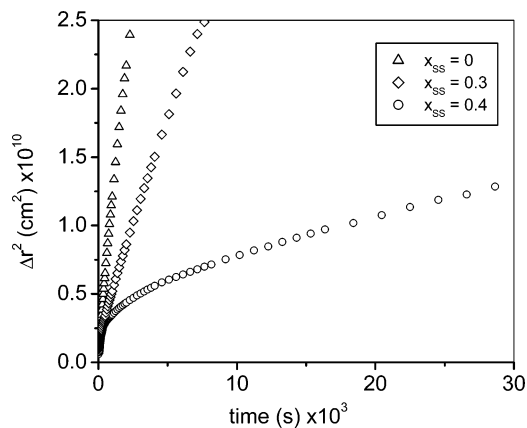


Figure 5. Evolution of the $\Delta r^2(t)$ of probe particles in CTAB micelles (100 mM) at different concentrations of the salt SS. Nonlinear variation is observed at $x_{SS} = 0.4$.

corresponds to a phase angle close to 30° . This implies a change in fluid microrheology from viscous to viscoelastic with increasing salt concentration. The above microrheological transitions are entirely analogous to the reported macrorheology of such wormlike micellar solutions.²³

Our analysis above underscores the qualitative agreement between micro- and macrorheology. It is worth discussing whether our microrheological approach (via DLS) is valid and if a further quantitative comparison can be made with macrorheological data. Taking the latter question first, a true comparison cannot be done because of the limited frequency ranges accessible in the two techniques. The lowest frequency accessible in the present study is about 1000 s^{-1} while the maximum accessible frequency in mechanical rheometry is limited to a few 100 s^{-1} . With respect to the validity of our approach, two pertinent questions that arise concern (a) the existence of inertial effects and (b) the assumption of continuum viscoelasticity. These questions have been addressed in detail by different groups.^{4,45} We tackle these below in the context of our study.

First, regarding inertial effects, the generalized Stokes–Einstein relationship does assume that inertial effects on the probe particles can be neglected. For particle inertia to be neglected, the viscoelastic penetration depth should be larger than the particle radius, a . For the motion of a particle of density ρ in a medium of modulus G , the above condition is satisfied for frequencies $\omega \ll \omega_{\text{max}}$, where $\omega_{\text{max}} = (9G/2a^2\rho)^{0.5}$. Here, we have $a = 100 \text{ nm}$ and $G \approx 10 \text{ Pa}$, which gives $\omega_{\text{max}} \approx 1 \text{ MHz}$. On the basis of this calculation, inertial effects can be safely ignored in our analysis. This is further evident from the weak dependence of $\tan \delta$ on frequency (Figure 4).

Next, for the assumption of continuum viscoelasticity to be valid, the probe particle radius should be larger than the characteristic mesh size (ξ) of entangled micelles. The mesh size can be determined either from small-angle neutron scattering (SANS) or from macrorheological measurements. For the surfactant concentration studied (100 mM), estimates of the mesh size range from ca. 20 nm (SANS) to ca. 45 nm (rheology).⁴⁶ Both of these are much less than the particle size used (100 nm). Thus, again, we can assume that the continuum assumption is valid for our particular experiment.

Finally, to understand the difference in microrheological response of CTAB micelles with different additives, the MSD of probe particles were measured in the presence of another organic salt SS. Figure 5 shows the MSD of probe particles in CTAB solutions at three different concentrations of SS. The

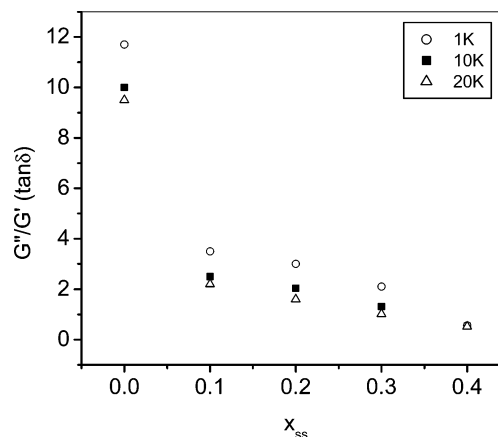


Figure 6. Variation in the ratio of G'' to G' (i.e., $\tan \delta$) at $\omega = 1000$, 10 000, and 20 000 s^{-1} as a function of x_{SS} . The behavior of the fluid becomes elastic in nature ($\tan \delta < 1$) at $x_{SS} = 0.4$.

changes in MSD are very similar to those observed for SPTS, with the shift to a nonlinear MSD occurring at a lower SS concentration compared to SPTS (compare the MSD at $x_{\text{salt}} = 0.4$ for SS and SPTS). Correspondingly, a plot of $\tan \delta = G''/G'$ as a function of x_{SS} at $\omega = 10\,000 \text{ s}^{-1}$ (Figure 6) indicates a rapid decrease at lower SS concentrations. This difference in microrheology may arise from the greater adsorption of SS on the surface of the micelles, thereby leading to faster growth of the micelles.

Conclusions

We have probed the microrheology of surfactant solutions in the presence of hydrophobic additives by monitoring the diffusion of probe particles using QELS. The MSD of probe particles embedded in micellar solutions is sensitive to the micellar structure. As the micelles change from spherical to wormlike upon addition of salts such as SPTS and SS, the MSD changes from linear to nonlinear. This nonlinearity reflects a transition from the viscous to viscoelastic nature of the fluid. The microrheological data at a given frequency can be used to compare the growth of micelles due to various additives. Differences in micellar growth are attributed to differences in hydrophobicity of the respective counterions and, in turn, their adsorption on the micelle surface.

Acknowledgment. The authors acknowledge helpful discussions with Professor Eric Kaler, University of Delaware.

References and Notes

- (1) MacKintosh, F. C.; Schmidt, C. F. *Curr. Opin. Colloid Interface Sci.* **1999**, *4*, 300.
- (2) Mason, T. G.; Weitz, D. A. *Phys. Rev. Lett.* **1995**, *74*, 1250.
- (3) Mason, T. G.; Ganesan, K.; van Zanten, J. H.; Wirtz, D.; Kuo, S. C. *Phys. Rev. Lett.* **1997**, *79*, 3286.
- (4) Gittes, F.; Schnurr, B.; Olmsted, P. D.; MacKintosh, F. C.; Schmidt, C. F. *Phys. Rev. Lett.* **1997**, *79*, 3286.
- (5) Schnurr, B.; Gittes, F.; MacKintosh, F. C.; Schmidt, C. F. *Macromolecules* **1997**, *30*, 7781.
- (6) Ziemann, F.; Radler, J.; Sackmann, E. *Biophys. J.* **1994**, *66*, 2210.
- (7) Amblard, F.; Maggs, A. C.; Yurke, B.; Pargellis, A. N.; Leibler, S. *Phys. Rev. Lett.* **1996**, *77*, 4470.
- (8) Langevin, D.; Rondelez, F. *Polymer* **1978**, *19*, 875.
- (9) Ullmann, G. S.; Ullmann, K.; Linder, R. M.; Phillis, G. D. *J. Phys. Chem.* **1985**, *89*, 692.
- (10) Nishio, I.; Reina, J. C.; Bansil, R. *Phys. Rev. Lett.* **1987**, *59*, 684.
- (11) Bucci, S.; Hoffmann, H.; Platz, G. *Prog. Colloid Polym. Sci.* **1990**, *81*, 87.
- (12) Madonia, F.; San Biagio, P. L.; Palma, M. U.; Schiliro, G.; Musumeci, M.; Russo, G. *Nature* **1982**, *302*, 412.
- (13) Phillis, G. D. J.; Clomenil, D. *Macromolecules* **1993**, *26*, 167.

- (14) Johnson, P. *Langmuir* **1993**, *9*, 2318.
- (15) Won, J.; Onyenezemu, C.; Miller, W. G.; Lodge, T. P. *Macromolecules* **1994**, *27*, 7389.
- (16) Rotsch, C.; Jacobson, K.; Radmacher, M. *Proc. Natl. Acad. Sci. U.S.A.* **1999**, *96*, 921.
- (17) Domke, J.; Radmacher, M. *Langmuir* **1998**, *14*, 3320.
- (18) Ma, H.; Jimenez, J.; Rajagopalan, R. *Langmuir* **2000**, *16*, 2254.
- (19) Crocker, J. C.; Valentine, M. T.; Weeks, E. R.; Gisler, T.; Kaplan, P. D.; Yodh, A. G.; Weitz, D. A. *Phys. Rev. Lett.* **2000**, *85*, 888.
- (20) Dasgupta, B. R.; Tee, S. Y.; Crocker, J. C.; Frisken, B. J.; Weitz, D. A. *Phys. Rev. E* **2002**, *65*, 051505.
- (21) Popescu, G.; Dogariu, A.; Rajagopalan, R. *Phys. Rev. E* **2002**, *65*, 041504.
- (22) Pine, D. J.; Weitz, D. A.; Chaikin, P. M.; Herbolzheimer, E. *Phys. Rev. Lett.* **1988**, *60*, 1134.
- (23) Rehage, H.; Hoffmann, H. *Mol. Phys.* **1991**, *74*, 933.
- (24) Magid, L. J. *J. Phys. Chem. B* **1998**, *102*, 4064.
- (25) Soltero, J. F. A.; Puig, J. E. *Langmuir* **1996**, *12*, 2654.
- (26) Hassan, P. A.; Candau, S. J.; Kern, F.; Manohar, C. *Langmuir* **1998**, *14*, 6025.
- (27) Hassan, P. A.; Yakhmi, J. V. *Langmuir* **2000**, *16*, 7187.
- (28) Buwalda, R. T.; Stuart, M. C. A.; Engberts, J. B. F. N. *Langmuir* **2000**, *16*, 6780.
- (29) Aswal, V. K.; Goyal, P. S.; Thiyagarajan, P. *J. Phys. Chem. B* **1998**, *102*, 2469.
- (30) Ait Ali, A.; Makhloufi, R. *Phys. Rev. E* **1997**, *56*, 4474–4478.
- (31) Hassan, P. A.; Valaulikar, B. S.; Manohar, C.; Kern, F.; Bourdieu, L.; Candau, S. J. *Langmuir* **1996**, *12*, 4350.
- (32) Cates, M. E. *Macromolecules* **1987**, *20*, 2289.
- (33) Cates, M. E. *J. Phys.: Condens. Matter* **1996**, *8*, 9167.
- (34) Rose, G. D.; Teot, A. S. In *Structure and Flow in Surfactant Solutions*; Herb, C. A., Prudhomme, R. K., Eds.; ACS Symposium Series 578; American Chemical Society: Washington, D.C., 1994; p 352.
- (35) Lin, Z. Q.; Mateo, A.; Zheng, Y.; Kesselman, E.; Pincallo, E.; Hart, D. J.; Talmon, Y.; Davis, H. T.; Scriven, L. E.; Zakin, J. L. *Rheol. Acta* **2002**, *41*, 483.
- (36) Hassan, P. A.; Manohar, C. *J. Phys. Chem. B* **1998**, *102*, 7120.
- (37) Phillies, G. D. J.; Lacroix, M. *J. Phys. Chem. B* **1997**, *101*, 39.
- (38) Streletzky, K. A.; Phillies, G. D. J. *J. Phys. Chem. B* **1999**, *103*, 1811.
- (39) Narita, T.; Knaebel, A.; Munch, J. P.; Candau, S. J.; Zrinyi, M. *Macromolecules* **2003**, *36*, 2985.
- (40) Sood, A. K.; Bandyopadhyay, R.; Basappa, G. *Pramana* **1999**, *53*, 223.
- (41) Cardinaux, F.; Cipelletti, L.; Scheffold, F.; Schurtenberger, P. *Europhys. Lett.* **2002**, *57*, 738.
- (42) van Zanten, J. H.; Rufener, K. P. *Phys. Rev. E* **2000**, *62*, 5389.
- (43) *Dynamic Light Scattering: Applications of Photon Correlation Spectroscopy*; Pecora, R., Ed.; Plenum Press: New York, 1985.
- (44) Israelachvili, J. N.; Mitchell, D. J.; Ninham, B. W. *J. Chem. Soc., Faraday Trans 2* **1976**, *72*, 1525.
- (45) Levine, A. J.; Lubensky, T. C. *Phys. Rev. Lett.* **2000**, *85*, 1774.
- (46) Koehler, R. D.; Raghavan, S. R.; Kaler, E. W. *J. Phys. Chem. B* **2000**, *104*, 11035.